

論文の内容の要旨

Oxidation-promoted interfacial synthesis of bis(diimino)metal

coordination nanosheets and their properties

(酸化的界面反応によるビス(ジイミノ) 金属
錯体ナノシートの合成と性質)

潘佳涵

Phua Jia Han Eunice

Introduction

Coordination nanosheets, or CONASHs, are two-dimensional molecular materials consisting of metal ions connected by bridging ligands via coordination bonds, which can be rationally designed and facilely synthesized in ambient conditions by a bottom-up method. This approach holds great promise for developing novel materials with unexpected and tailorable properties based on the intrinsic nature of the electron delocalization over the infinite plane when strongly correlated electron systems are constructed using an appropriate combination of transition metals with π -conjugated bridging ligands. The bottom-up approach of synthesizing two-dimensional (2D) coordination nanosheets (CONASHs) from their corresponding metal ions and organic ligands has proved its potential to form versatile and highly functional materials based on the redox-active, electrochromic, electro-conductive, photo-conductive, luminescent, catalytic, photo-electro conversion, and electrocapacitive properties as some of its examples.

Previous research on bis(dithiolato)nickel (**NiDT**) nanosheet afforded film-like products with a kagome lattice and controllable thickness down to single-layer using facile gas/liquid and liquid/liquid interfacial coordination reactions. Their strongly correlated electronic properties include high electronic conductivity of $160 \text{ S}\cdot\text{cm}^{-1}$ and the prediction of single-layer **NiDT** to be a 2D topological insulator. Chapter 1 of this dissertation elaborates on the background as well as the potential of this research and the aim of the research.

Previous work

By coordinating metal ions and their ligands at the calm interface of two immiscible solutions, the liquid/liquid interfacial reaction has been previously utilized as a convenient and relatively simple method of synthesizing such bottom-up coordination nanosheets. Previously, the electronic analogue of **NiDT** formed by a similar liquid/liquid interfacial reaction using the hexaaminobenzene trihydrochloride (**HAB** \cdot 3HCl) ligand and aqueous ammonia in

water and bis(penta-2,4-dionato)nickel(II), $\text{Ni}(\text{acac})_2$ has been investigated. However, the system gave rather drastically different results when carried out under inert conditions and in atmospheric conditions. It was then hypothesized that oxidation is required for the formation of the resulting bis(diimino)nickel(II) (**NiDI**) CONASH.

Chemical synthesis of **NiDI**

To make use of the oxidation requirement, the usual liquid/liquid interfacial system was modified. The optimized synthesis of the **NiDI** nanosheet formation was performed through an oxidation assisted reaction between the **HAB**·3HCl ligand (0.4 mM) and nickel(II) acetate (15 mM) in 4.5 M excess concentrated ammonia solution.

The plausible mechanism is as-proposed in Fig. 1a. In the as-prepared solution, two **HAB** ligands neutralized by ammonia reversibly coordinate to the nickel ion due to the weak coordination ability of anilines. As dioxygen is introduced, a pair of the ligand's coordinated amines undergoes oxidation, which dramatically improves the coordination ability, resulting in a stabilized π -conjugated five-membered metallacycle. Henceforth, the other free amines on the ligand similarly coordinate to other nickel ions, which are sequentially coordinated with other ligands. Eventually, the complexes expand to become a large crystalline **NiDI** nanosheet with a metallic luster on the gas/liquid interface as seen in Fig. 1b. This sheet forms a kagome lattice similar to the illustration in Fig. 1a. Thicknesses of the crystalline black sheets depend on the rates and amount of dioxygen introduced into the gas phase just above the reaction solution.

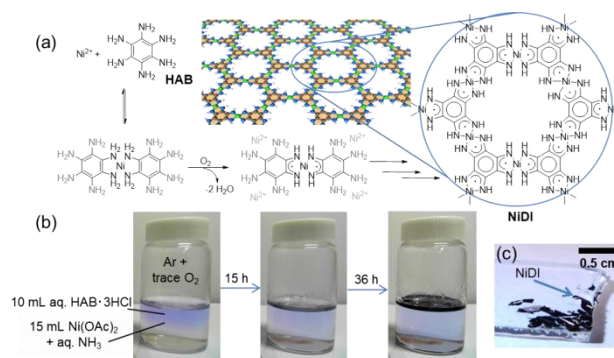


Figure 1. Formation of chemical synthesized **NiDI**. (a) Mechanism of **NiDI** formation and the resulting kagome lattice. (b) Reaction conditions and gradual formation of **NiDI** sheet on aqueous surface with oxidation. (c) Crystalline **NiDI** transferred onto glass substrate.

The metallic lustre of thicker nanosheets indicates a certain level of crystallinity of the **NiDI** CONASH. This novel sheet is slowly formed on the calm liquid surface over time, as oxygen is required for the formation. This is due to the need for the biradical formation with structures similar to bis(*o*-diiminobenzosemiquinonato)nickel(II), $\text{Ni}(\text{isq})_2$ (*isq* = *o*-diiminobenzosemiquinonate), which has been synthesized under air. The slow exposure to atmospheric oxygen is the crux for the high crystallinity of the sheets formed. With this gas/liquid interfacial reaction method based on the previous interfacial synthesis, large centimetre-scale **NiDI** nanosheets with high crystallinity visible to the naked eye as seen in Fig. 1c can be obtained.

Characterizing the **NiDI** sheets using X-ray photoelectron spectroscopy (XPS) and IR proved the formation of the neutral **NiDI** nanosheet. Powder X-ray diffraction (PXRD) analysis of the bulk **NiDI** sheet obtained using high energy synchrotron radiation gave distinct peaks, which further proved the crystallinity of the product formed. These peaks were found to match the simulation data of an eclipsed nanosheet array with the crystal lattice parameters of $a = b = 13.01 \text{ \AA}$ and $c = 3.25 \text{ \AA}$. 1 cm^2 of thick **NiDI** sheets can be easily synthesized and characterized using SEM and TEM. By controlling the rates and amount of dioxygen, differing thicknesses of **NiDI** were obtained as observed by AFM. Partly due to the limitations of AFM, the thickest film measured was

2.7 μm , corresponding to more than three thousand layers. With the reduction of exposure time to dioxygen, the thickness of the **NiDI** sheets detected was reduced from approximately 20 nm-thick to just 0.8 nm-thick at its edges, corresponding to the first detection of a single layer **NiDI** nanosheet.

Electrical conductivity of chemically synthesized **NiDI** nanosheet in its pelletized form was measured using a four-terminal method under helium while varying the temperature. The electrical conductivity (σ) of the **NiDI** nanosheet increased with temperature and was $1.3 \times 10^{-3} \text{ S}\cdot\text{cm}^{-1}$ at 298 K, indicating its semiconducting nature with the activation energy of 0.16 eV. Magnetic investigations of the chemically prepared **NiDI** nanosheet using superconducting quantum interference device (SQUID) revealed the existence of non-negligible magnetic moments, while neutral $\text{Ni}(\text{isq})_2$, a fundamental constituted unit of the **NiDI** nanosheet, forms a non-magnetic singlet state. The detailed synthesis, characterization and discussion about the chemically synthesized **NiDI** CONASH is given in Chapter 2 of this dissertation.

Electrochemical synthesis of **NiDI**

Discovering the necessity for oxidation, another synthetic method using electrochemical oxidation, which produces the **NiDI** nanosheet directly on an electrode surface, was developed. The electrochemical polymerization was carried out at an indium-tin oxide (ITO) glass in a **HAB**·3HCl-Ni(OAc)₂-NH₃ aqueous solution with 0.1 M NaBF₄ as electrolyte under an argon atmosphere (Fig. 2a). A black film immediately formed and adhered strongly to the ITO electrode when 0.56 V vs. Ag/AgCl was applied to oxidize **HAB**. In comparison, electro-oxidation of nickel-free reaction solution (**HAB**·3HCl-NH₃-NaBF₄) afforded no film on the electrode, indicating the role of nickel ions for the polymerization. The electrochemically prepared black film identified by XPS, IR and PXRD, confirms an identical chemical structure with the chemically synthesized **NiDI** nanosheet but with lower crystallinity. This less ordered structure of electrochemically prepared **NiDI** results from the quick formation and the difference of the reaction field (solid-liquid interface for the electropolymerization versus gas-liquid interface for the chemical polymerization). It is postulated that this electropolymerization proceeds through an identical mechanism with the dioxygen-assisted sheet formation.

This electrochemical method enables a more controllable growth of the nanosheet as compared to the gas-liquid interfacial reaction as the degree of oxidation can be precisely adjusted. A series of samples with synthetic times varying from 10 s to 60 s were synthesized (Fig. 2b), and their UV-vis-NIR spectra and AFM images were obtained. Representative scratched samples with synthetic times of 20 s, 40 s and 60 s, show non planar and jagged surfaces from their AFM topographical images. The empty spaces (blank ITO without **NiDI**) decreased while the topographical height increased gradually with time. This indicates the growth of perpendicularly deposited **NiDI** nanosheets which is as illustrated by the illustration below each of the height profiles (Fig. 2c). After 60 s, the average thickness of the **NiDI** film was 75 nm.

UV-vis-NIR absorption spectra exhibit a broad peak over 700 – 1500 nm with $\lambda_{\text{max}} = \text{ca. } 1060 \text{ nm}$. The absorbance of the respective samples at 1060 nm increases non-linearly with time, corresponding to the charge vs time graph for each of the respective samples during cyclic voltammetry, as well as the gradual increase of the

charge consumed during their syntheses. This non-linear increase corresponds to the hypothesis of the perpendicular growth of **NiDI** on the ITO electrodes.

Chemical and Physical Properties

Redox activities of both chemically and electrochemically synthesized **NiDI** nanosheets were investigated using cyclic voltammetry (CV) in 1 M $\text{Bu}_4\text{NClO}_4\text{-MeCN}$. The chemically prepared **NiDI** nanosheet exhibits peak couples ascribed to the same $[\text{NiDI}]^+ / [\text{NiDI}]^0$ couple based on the redox behavior of the mononuclear bis(diimino)nickel complex, indicating the chemical reversibility of the **NiDI** nanosheet. Cyclic voltammograms of electrochemically prepared **NiDI** nanosheet on ITO exhibits not only faradaic currents but also very large charging currents. Representative CV spectra plotted together show an increase in the charge capacity with the increase in synthetic time, which also means an increase in charge capacity with the amount of **NiDI**. This, together with its stable redox behavior and electrical conductivity, reveals its potential for applications for charge storage materials. Chapter 3 of this dissertation explores about the synthesis, characterization, as well as the investigations of the electrochemically synthesized **NiDI** nanosheet.

Expanding to Other Metal Ion Systems

Chapter 4 of the dissertation then explores the advantage of synthesizing the sheets using the bottom-up method. Using the same chemical method which utilizes ambient oxygen for synthesis, new systems were investigated by changing the nickel ion source to other metal sources. New systems involving Group 10 elements were investigated and characterized. Due to the nature of these new systems, some of the characterization of the new systems proved to be difficult. However, some of their novel physical properties were still investigated, which were found to be different from that of the **NiDI**. These findings and a discussion of the new systems formed are given in Chapter 4.

The concluding remarks and the research perspectives are then given in Chapter 5, the final chapter.

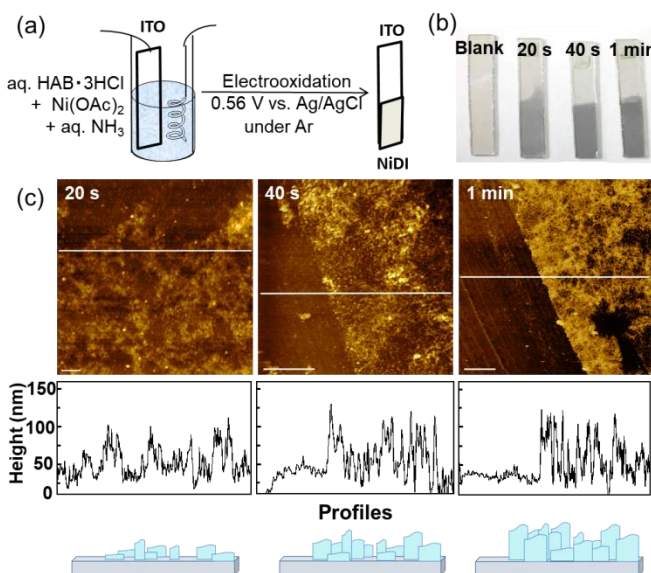


Figure 2. Synthesis and characterization of electrochemically synthesized **NiDI**. (a) Illustration of electrochemical setup of constant potential synthesis of **NiDI** on ITO. (b) Photo of blank ITO as compared to **NiDI** samples which has undergone 20 s, 40 s and 1 minute of constant potential of 0.56 V vs Ag/AgCl. (c) Illustrations, AFM topography images and height profiles of scratched AFM samples obtained by 0.56 V for 20 s, 40 s and 1 minute respectively. Scale bars represent 5 μm .